Monatshefte für Chemie 137, 647–655 (2006)
DOI 10.1007/s00706-006-0443-y

Monatshefte für Chemie
Chemical Monthly
Printed in Austria

Photocatalytic TiO_2 Coatings: Effect of Substrate and Template[#]

Urška L. Štangar[1,*], **Urh Černigoj**[1], **Polonca Trebše**[1], **Ksenija Maver**[1], and **Silvia Gross**[2]

[1] Laboratory for Environmental Research, Nova Gorica Polytechnic, P.O.B. 301, 5001-Nova Gorica, Slovenia
[2] CNR-ISTM, University of Padova, I-35131 Padova, Italy

Received December 2, 2005; accepted (revised) January 9, 2006
Published online March 2, 2006

Summary. Transparent TiO_2 films with a high photodegradation activity towards an azo dye in aqueous solution were prepared by sol–gel processing. Films on soda–lime glass supports protected with a thin silica barrier layer exhibited better crystallization and monodisperse nanoparticles, higher absorption of light below 370 nm, and higher photocatalytic activity than those films deposited on bare glass supports proving the detrimental effect of interdiffused sodium ions on the development of the anatase nanostructure. The effect of substrate was more pronounced in thinner films (300 nm) than in thicker ones (1200 nm), which were achieved by adding a template (*i.e.* Pluronic F127) to the sol.

Keywords. Sol–gel titania; Surfactants; Optical properties; Photodegradation; Structure-activity relationships.

Introduction

Titanium dioxide has become the material of choice for hydrophilic self-cleaning and photocatalytically active surfaces in general [1, 2]. This is because it displays several desirable features of an ideal semiconductor photocatalyst ($E_g = 3.2$ eV): it is chemically and biologically inert, photocatalytically active in the UV component of sunlight, inexpensive, and may be easily produced. In this framework, the sol–gel technique has emerged as one of the most promising techniques for growing TiO_2 thin films.

The good photoefficiency of the titania films relies also on the high contact surface area exposed to organic pollutant molecules and on their nanocrystalline structure [*e.g.* 3, 4], which facilitates efficient photoinduced electron-hole pair

* Corresponding author. E-mail: urska.lavrencic@p-ng.si
[#] Dedicated to Prof. *Ulrich Schubert* on the occasion of his 60th birthday

generation with a sufficient charge separation. The film structure and morphology could be tailored through the variation of the sol–gel processing conditions and the use of structure directing agents, *i.e.* templates. Their role is to create porosity, smaller particles, and a larger surface area of the material, which would lead to improved photoefficiency. According to many reports, the best performing particles for photocatalysis are anatase nanocrystals with hydroxyl groups on their surface [1].

An important factor that determines the photocatalytic efficiency of titania films is the type of the substrate. The detrimental effect of sodium contamination – originating from the soda–lime glass substrates during heat treatment – has already been investigated. In this regard, various explanations were given, such as: (i) Na^+ ions raise the temperature of anatase formation and increase the particle size [5], (ii) they promote the recrystallization of the anatase to rutile [6], (iii) they perturb the crystallinity of TiO_2 [7], prevent the formation of the anatase phase, and produce recombination centers of photogenerated electron-hole pairs [8], (iv) they produce either sodium titanate ($Na_2O \cdot xTiO_2$) or a brookite phase [8, 9], (v) they cause bonding or a shift of the oxygen anions resulting in the partial reduction of Ti(IV) to Ti(III) [10], and finally (vi) they adsorb CO_2 in air to form carbonate and cause the increase in the carbon amount [11].

In this work we studied the effect of the substrate (soda–lime glass with or without protecting thin silica film) and of the template (triblock copolymer Pluronic F127) on the structure, morphology, and photoefficiency of our sol–gel produced titania films. The optical properties, structure, and morphology of the material were investigated by UV-VIS spectroscopy, X-ray diffraction analysis, X-ray photoelectron spectroscopy, and atomic force microscopy, while photoefficiency of various films was determined by *in situ* UV-VIS spectroscopy. The aqueous solution of the azo dye Plasmocorinth B served as a photodegradation medium [12] since in the absence of a photocatalyst this dye is very stable under UV light and environmental conditions.

Results and Discussions

Optical Properties

All titania films obtained after calcination were of a high optical quality. They were crack-free and transparent over the whole visible spectral range (Fig. 1). In our previous study [12] it has been shown that the type of the substrate (bare glass or SiO_2-coated glass) has no influence on the thickness of the titania films. On the other hand we showed that the addition of a templating surfactant in the sol results in a thicker film obtained by the same number of dipping-heating cycles. The thickness of films D (without surfactant) in Fig. 1 is about 300 nm, while the films C (with Pluronic F127) are much thicker – 1200 nm. Both types of films were deposited by four dipping-heating cycles.

UV-VIS transmittance spectra of various films (Fig. 1) are characterized by interference fringes with lower amplitudes in case of templated films (spectra C4S and C4N). Such phenomena in UV-VIS spectra can be ascribed to the change in density and hence in porosity of the film structure [12, 13]. In addition, inter-

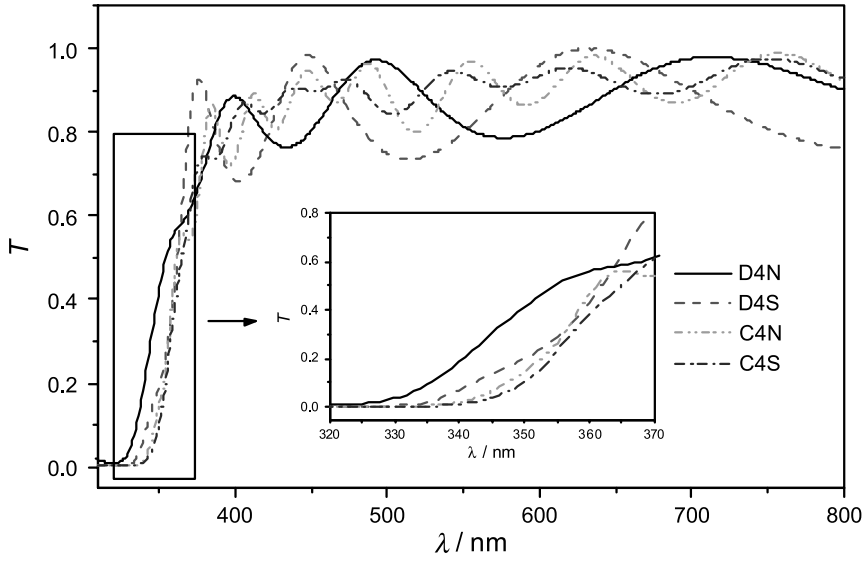

Fig. 1. UV-VIS transmittance spectra of different TiO_2 films

ference fringes may vary inside one particular spectrum suggesting that films are multilayers with various refractive indices.

When comparing spectra of the two films D (spectra D4S and D4N), it is clearly seen that the protecting thin silica film underneath caused a red-shift of the absorption edge of the upper titania film. Absorption of light below 370 nm (Fig. 1, inset) is due to the excitation of electrons from the valence band to the conduction band of TiO_2. As the films' thickness was the same in both cases, this gave evidence that type of the substrate played a significant role in the absorption of light below 370 nm and hence also in the photocatalytic activity of TiO_2 films (described in the following subchapter).

In contrast to spectra of films D, the two spectra of films C in Fig. 1 do not differ significantly in the UV absorption properties (there is not such a significant shift of the absorption edge). This is because the effect of the substrate was diminished in case of thicker films C (1200 nm). A further red-shift of the absorption edge of films C when compared to films D, deposited on the same kind of substrate, can be explained with a higher film thickness and with a difference in crystallites within the films due to the addition of the template.

Photocatalytic Efficiency

An aqueous solution of Plasmocorinth azo dye (chemical structure is shown in Fig. 2 – inset) was used for *in situ* photodegradation studies in the home-made continuous flow cell [12]. Figure 2 shows photobleaching curves – absorbance at 526 nm as a function of irradiation time – of the dye solution in contact with TiO_2 films deposited by four dipping-heating cycles from sol D and from sol C on the two types of substrates. The correlation between a red shift of the absorption edge in the UV-VIS transmittance spectra (Fig. 1) and the photodegradation efficiency (Fig. 2) is clearly evident. The most striking difference was found again when

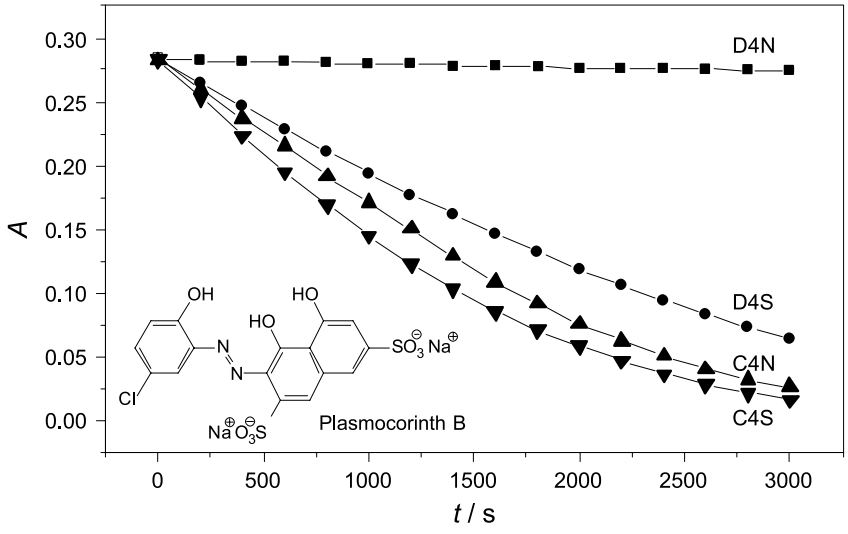

Fig. 2. Photobleaching of Plasmocorinth B solution (absorbance at 526 nm *vs*. irradiation time) in contact with different TiO_2 films

comparing the photobleaching curves of the two films D (D4N, D4S). The substrate has a big impact here as the films D4 are still relatively thin (300 nm). When deposited on bare soda–lime glass (D4N) they were totally inactive – the surrounding dye solution remained stable during the irradiation. When deposited on soda–lime glass with a protecting SiO_2 layer (D4S), films showed a considerable photoactivity, which is in accordance with a significant red shift of the UV-VIS absorption edge.

As expected, both samples C exhibited higher photodegradation rates and the observed difference between them was small (lines C4N, C4S). This is again due to much lower effect of the substrates when the films are thick enough. The dye solution in contact with templated films C was almost completely discolored in less than 1 hour of irradiation. The photocatalytic activity of our films was compared also with that of commercially available Pilkington Activ^{TM} self-cleaning glass, but the latter was almost inactive under our experimental conditions (only 5% of Plasmocorinth B were decomposed after 3000 s). This remains unclear and shows that the use of a standard photocatalytic layer as a reference film cannot be generalized to all different photodegradation experiments, performed either in liquid or gas phase.

The photocatalytic activity was evaluated also as formal quantum efficiency (FQE), which is defined as rate of disappearance of the organic molecule divided by the incident photon flow (Φ_p) [1c]. Φ_p for the wavelength range 335–510 nm was in our photocatalytic cell $7.17 \times 10^{17}\ s^{-1}$, which was determined by potassium ferrioxalate actinometry [14]. FQE was found to be 0.009% for D4S film and 0.017% for C4S film. It should be noted that the majority of the photons included in Φ_p (the photons with the wavelengths above 385 nm and photons that are absorbed by the dye solution) are not absorbed by the titania film and therefore the FQE value is much lower than the photonic efficiency or quantum yield would be [1c].

Structural and Morphological Properties

A clear relationship between the optical properties and the photocatalytic efficiency should reflect also in the structural/morphological properties of various TiO_2 films. X-Ray diffraction (XRD) patterns of the most efficient films C are presented in Fig. 3a. In order to get diffractograms with higher intensities of peaks and therefore better identification of the crystalline phases, they were recorded by using the "film powder" samples (instead of immobilized thin films). We obtained them by mechanical scratching a number of calcined C4 films away from their substrates until the amount of powder gained in such a way was sufficient for XRD measurements. Figure 3a shows that films C4 with high photocatalytic activities consist of a predominant anatase crystalline phase, which is also supposed to be the most active one for photocatalytic reactions [1]. In addition, the presence of a brookite phase [15] with a small peak at $2\theta = 30.8°$ is evident in both samples. Films were calcined at 500°C, which was high enough for the formation of the

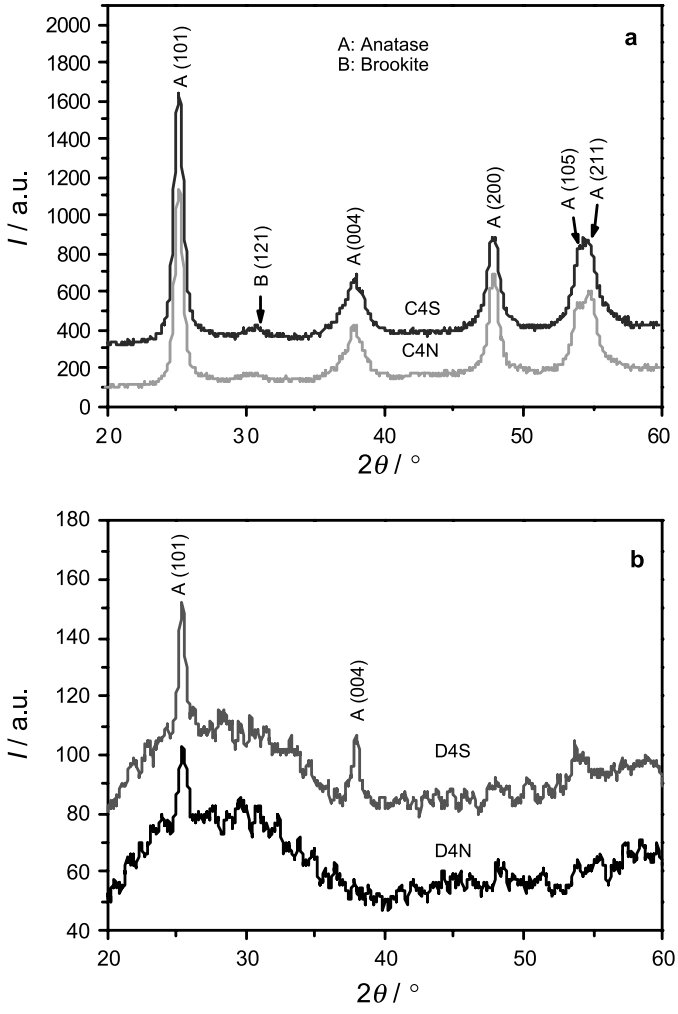

Fig. 3. XRD patterns of TiO_2 film powder samples (a) and thin film samples (b)

active anatase phase and low enough that the conversion to rutile was negligible. It has been found that TiO_2 particles immobilized on the quartz support during calcination remained in the anatase form even at 800°C, whereas self-supported TiO_2 particles in powders were more easily converted into the rutile form, starting already at 500°C [16]. Accordingly, we observed 5–30% of rutile phase relative to anatase when the samples were calcined in a powder form [12].

Similarly to UV-VIS and photocatalytic results, the XRD patterns of both C4 films (Fig. 3a) show only small differences. The effect of the glass support on relatively thick TiO_2 coatings (1200 nm) was minor: the most noticeable was the intensity decrease of the major anatase-TiO_2 (101) peak at $2\theta = 25.4°$ by 21% in the sample C4N compared to C4S. In spite of small differences, this is an indication that type of the substrate has an influence on the anatase crystal growth. To verify it, we looked at thinner C1 films (deposited by only single dipping, film thickness ~300 nm) with atomic force microscopy (Fig. 4). The AFM images undoubtedly prove the effect of the substrate on the crystal growth. Sodium ions migration from the substrate without a barrier film in the interior of TiO_2 film (C1N) prevents the formation of granular surface with well-resolved nanoparticles as it is in the case of using substrate with a silica barrier film (C1S). The presence

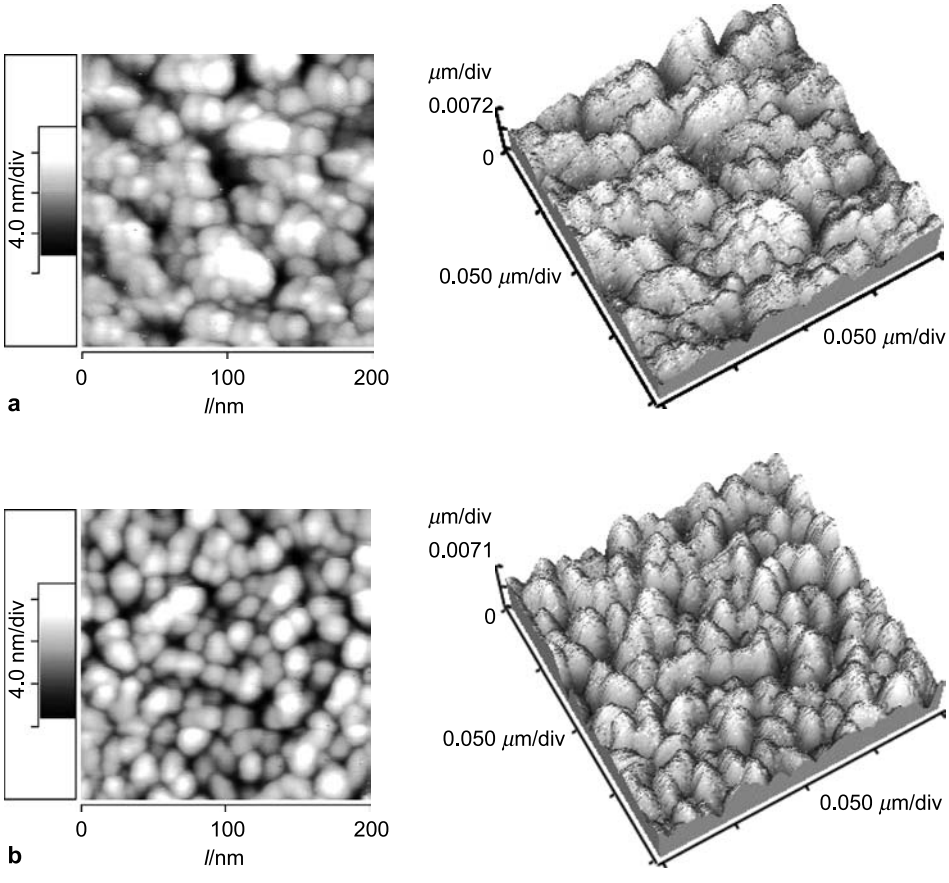

Fig. 4. AFM 2- and 3D images of the surface of TiO_2 films C1N (a) and C1S (b)

of Na^+ ions causes the agglomeration/aggregation of particles, which resulted in lower contact surface area and therefore in lower photodegradation rates.

The films D4 were not characterized by XRD measurements like films C4, in film powder form, mainly for two reasons: (i) their thickness is four times lower and the collecting of powder would be very time consuming, (ii) the adherence of films D to the glass support is very high and therefore the mechanical scratching extremely difficult. XRD measurements were done directly on immobilized films resulting in less intense diffraction peaks and noisy patterns (Fig. 3b). Despite this the significant differences between D4N and D4S films are evident. The crystallization of anatase in case of D4N is considerably less developed, *i.e.* the amorphous-anatase TiO_2 transition is incomplete. This is in a good correlation with photocatalytic inactivity of D4N films (Fig. 2).

Our results confirm that sodium ions impurities have a negative influence on the crystallization of TiO_2, which is otherwise very important for photocatalysis utilizing the semiconducting properties of the material. We agree with the somehow contradictory explanation that sodium ions retard the formation of the anatase phase and increase the particle size [5] in the sense that Na^+ ions inhibit anatase crystallization and cause agglomeration of TiO_2 particles. However, investigation on our films did not give evidence that sodium ions would stimulate the crystallization of any other phase. The brookite phase was found in the thin film samples regardless of the type of the substrate.

The surface and in-depth composition of films D1N, D1S, and C1S were analyzed also by X-ray photoelectron spectroscopy (XPS) to investigate the chemical composition of the deposited layers, their possible intermixing (in the case of S substrates), and the interdiffusion of sodium in the coatings. To this aim, depth profiles were measured and the quantitative distributions of the elements as a function of the depth were compared. By comparing D1N and D1S samples, the most evident difference is the different amount of detected sodium. While in D1N the atomic percentage of Na is quite high (*ca.* 5–6%) and constant along the sputtered layer, in the sample D1S the sodium content is lower than 0.5%, proving the effectiveness of the silica barrier film. After 80 minutes of sputtering, the approaching of the boundary between titania film and the underlying silica layer was evidenced by a decreasing atomic percentage of titanium and by the corresponding increasing intensity of the silicon signal. No signal ascribed to silicon could be evidenced along the film thickness up to 80 minutes sputtering, whereas afterwards, a significant intermixing of silica and titania was observed. Along the film thickness, titanium atomic percentage ranges in the interval 30–35%, and oxygen amount, according to titania stoichiometry, spans the range 60–65%. In Fig. 5, the survey spectra of the sample before sputtering and after 80 minutes of erosion are superimposed. Whereas in the not-sputtered sample the carbon signal is still evident together with titanium and oxygen peaks, in the second survey, the carbon signal is strongly reduced, while the peaks of the underlying silica layer could be evidenced.

As far as the sample C1S is concerned, the XPS in-depth profile again reveals the presence of a compositionally pure and completely Na-free titania layer, while the underlying silica layer is characterized by a presence of sodium ranging between 1–2%. Also in this case, a noticeable intermixing of titania and silica

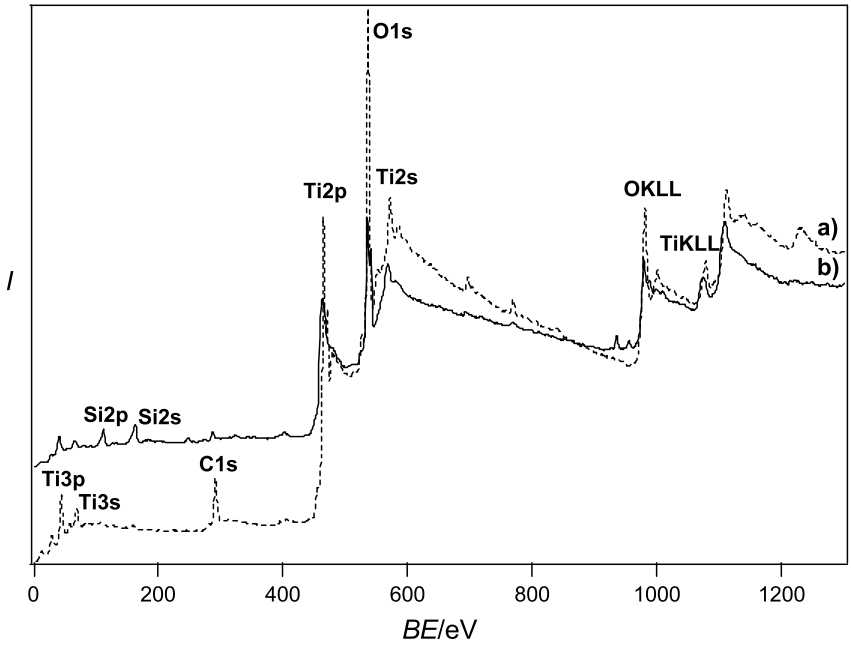

Fig. 5. Superimposed XPS survey of sample D1S on the surface (a) and after 80 minutes of sputtering (b)

was evidenced by the XPS depth profile, since after 130 minutes of sputtering both increasing silicon signal and decreasing titanium signal are present.

It should be underlined that in all the analyzed samples, especially in the outmost layers, the O1s peak is characterized by a major component at 530.0 eV, ascribed to titania [17], and by a shoulder at about 531.8 eV, which was attributed to a hydroxylated Ti–OH species [11].

Experimental

Titania sols and coatings were made according to Ref. [12] from a modified $Ti(OPr^i)_4$ with ethyl acetoacetate and 2-methoxyethanol, in the presence or absence of non-ionic surfactant $PEO_{100}PPO_{65}$ PEO_{100} (Pluronic F127, Sigma). Films were deposited by the dip-coating technique on soda–lime glass plates with or without a barrier silica layer and then heat-treated at 500°C for 30 min. Silica films were prepared from $Si(OEt)_4$, ethanol, HNO_3, and H_2O [12] by a single dipping and heating at 500°C for 30 min. The names of the samples in this study are composed of three characters: (1) D = made without surfactant or C = made with Pluronic F127, (2) 1 or 4 = number of dipping-heating cycles, and (3) N = deposited on bare glass support or S = deposited on glass support with a thin silica film.

The thickness of the films was measured on a Taylor-Hobson Talysurf profilometer. UV-VIS spectra of the films and the dye solutions were recorded on a Hewlett-Packard 8453 UV-VIS spectrophotometer. A detailed procedure of the photocatalytic experiment is described in Ref. [12]. XRD measurements were made with a Philips PW1710 automated X-ray diffractometer using graphite monochromatized Cu–Kα radiation in the step-by-step mode. Surface topography of TiO_2 films was evaluated by AFM on a CP-II scanning probe microscope (Veeco) in non-contact mode at constant force in air. The surface and in-depth composition of films were analyzed by XPS on a Perkin-Elmer Φ 5600ci spectrometer.

Acknowledgements

We are grateful to Prof. *P. Lianos* for valuable discussions and reference titania films, to Prof. *V. Kaučič* and *E. Kranjc* for XRD measurements, to *A. Zattin* for technical support, and to the Slovenian *Ministry of Higher Education*, *Science and Technology* for financial support. A special thank from the first author goes to Prof. *U. Schubert* and Prof. *N. Hüsing* for hospitality at Vienna University of Technology and introduction to surfactant-assisted sol–gel processing.

References

[1] For reviews see: a) Parkin IP, Palgrave RG (2004) J Mater Chem **15**: 1689; b) Kaneko M, Okura I (2002) Photocatalysis: Science and Technology. Springer; c) Mills A, Le Hunte S (1997) J Photochem Photobiol A: Chem **108**: 1; d) Carp O, Huisman CL, Reller A (2004) Prog Solid State Chem **32**: 33; e) Diebold U (2003) Surface Sci Reports **48**: 53
[2] Allen NS, Edge M, Sandoval G, Verran J, Stratton J, Maltby J (2005) Photochem Photobiol **81**: 279
[3] Stathatos E, Lianos P, Tsakiroglou C (2004) Microporous Mesoporous Mater **75**: 255
[4] Yu JC, Wang X, Fu X (2004) Chem Mater **16**: 1523
[5] Nam HJ, Amemiya T, Murabayashi M, Itoh K (2004) J Phys Chem B **108**: 8254
[6] Trapalis CC, Keivanidis P, Kordas G, Zaharescu M, Crisan M, Szatvanyi A, Gartner M (2003) Thin Solid Films **433**: 186
[7] Guillard C, Beaugiraud B, Dutriez C, Herrmann JM, Jaffrezic H, Jaffrezic-Renault N, Lacroix M (2002) Appl Catalysis B: Environmental **39**: 331
[8] a) Paz Y, Luo Z, Rabenberg L, Heller A (1995) J Mater Res **10**: 2842; b) Paz Y, Heller A (1997) J Mater Res **12**: 2759
[9] Kuznetsova IN, Blaskov V, Stambolova I, Znaidi L, Kanaev A (2005) Mater Lett **59**: 3820
[10] Yu J, Zhao X, Zhao Q (2001) Mater Chem Phys **69**: 25
[11] Yu JC, Yu J, Zhao J (2002) Appl Catalysis B: Environmental **36**: 31
[12] Černigoj U, Lavrenčič Štangar U, Trebše P, Opara Krašovec U, Gross S (2006) Thin Solid Films **495**: 327
[13] Iketani K, Sun RD, Toki M, Hirota K, Yamaguchi O (2003) J Phys Chem Solids **64**: 507
[14] Murov SL, Carmichael I, Hug GL (1993) Handbook of Photochemistry (second ed.). Marcel Dekker Inc., New York, pp 299–305
[15] JCPDS of TiO_2: anatase 21-1272, brookite 29-1360, rutile 21-1276
[16] Martyanov IN, Klabunde KJ (2004) J Catal **225**: 408
[17] a) Seah MP (1990) In: Briggs D, Seah MP (eds) Practical Surface Analysis, vol. 1 J Wiley & Sons, p 543; b) Moulder JF, Stickle WF, Sobol PE, Bomben KD (1992) In: Handbook of X-Ray Photoelectron Spectroscopy. Perkin Elmer Corporation, Eden Prairie, MN